

Conductive mode imaging of thermistor grain boundaries

J. Seaton, C. Leach*

Manchester Materials Science Centre, University of Manchester and UMIST, Grosvenor Street, Manchester M1 7HS, UK

Abstract

PTC thermistors undergo a rapid increase in grain boundary resistivity, covering several orders of magnitude, at temperatures just above the Curie temperature, T_C , which is associated with a ferroelectric to paraelectric phase transformation. In this study, hot-stage conductive mode scanning electron microscopy has been used to investigate the characteristics of individual thermistor grain boundaries over a range of temperatures around T_C . Using the remote electron beam induced current (REBIC) configuration, imaging has revealed EBIC contrast consistent with the presence of negatively charged electrostatic grain boundary barriers for the first time in a commercial thermistor. Not all grain boundaries within the thermistor were found to be EBIC active and the EBIC contrast was only observed at temperatures above T_C . EBSD analysis of grain boundary crystallography indicated that the EBIC active grain boundaries were predominantly high angle.

© 2003 Elsevier Ltd. All rights reserved.

Keywords: BaTiO₃; Conductive mode; Electron microscopy; Grain boundaries; Thermistor

1. Introduction

Positive temperature coefficient (PTC) thermistors based on polycrystalline sintered n-type semiconducting BaTiO₃ show a large, reproducible increase in grain boundary resistivity, frequently in excess of five orders of magnitude, at temperatures just above the ferroelectric to paraelectric phase transformation, which occurs at ~ 130 °C in undoped BaTiO₃. This characteristic is exploited in a variety of applications, including telecommunications based current surge protection devices, self-regulating heater elements and temperature sensors.

Early models for the PTC effect linked the rapid increase in the grain boundary barrier height just above the transformation, or Curie, temperature (T_C) to a sudden decrease in the dielectric constant.^{1,2} These models were developed further by considering effects due to spontaneous polarisation and charge shielding, as well as the influence of secondary grain boundary phases and trap state activation.^{3–5} More recently, studies have reported variability in the magnitude and form of PTC response at individual grain boundaries, which have been linked to differences in grain boundary misorientation at the interface.^{6,7}

1.1. Conductive mode microscopy

Conductive mode microscopy is a mode of operation of the SEM that is widely used to study electrically active grain boundaries in polycrystalline semiconductors and electroceramics.^{8–11} It complements other, more established, techniques, such as Impedance Spectroscopy, in two main ways. Firstly it is a local property technique, providing information about the electrical characteristics of individual grain boundaries, rather than bulk-averaged properties. Secondly, quantitative analysis of the signal can yield additional information about the grain boundary electrical structure including the depletion region width, and diffusional parameters necessary to understand the field dependence of the barrier height, as well as distinguishing between conducting and intrinsic regions. Fig. 1 shows the experimental configuration, in which two ohmic current collecting electrodes are positioned on either side of the area being studied, enabling any currents generated within the specimen by the impinging electron beam to be collected and amplified to form the image. Depending on the type of signal information being sought, the electrodes generally either have a wide separation (several grain widths apart on the surface) in what is termed the remote electron beam induced current (REBIC) configuration, or are located on adjacent grains on either side of a single grain boundary in the grain boundary–electron beam induced current (GB–EBIC) configuration.

* Corresponding author. Tel.: +44-161-200-3561; fax: +44-161-200-3586.

E-mail address: colin.leach@man.ac.uk (C. Leach).

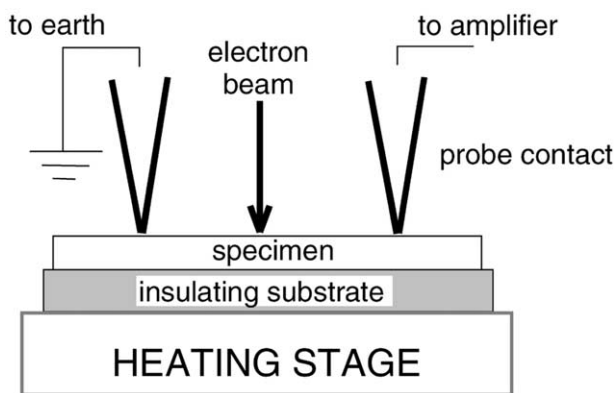


Fig. 1. Specimen configuration for conductive mode microscopy.

Three forms of conductive mode contrast have been identified in electroceramics. These are resistive contrast, β -conductivity contrast and EBIC contrast. The type of contrast that is observed at a particular grain boundary is sensitive to its electrical characteristics and can be used to infer details of the interfacial structure. For example, resistive contrast arises because the inter-electrode region of the specimen acts as a current divider to the absorbed primary beam current as it travels to earth. Consequently, localised changes in specimen resistivity are seen as perturbations to a background brightness gradient.⁸ β -conductivity arises from an enhanced current flow between the electrodes under an applied bias and is caused by local increases in conductivity arising from the injection of mobile charge carriers by the primary electron beam.¹² EBIC contrast is due to the separation and collection of beam generated electron-hole pairs by the depletion fields present on either side of a charged grain boundary.¹¹ Since electrostatic barriers form at thermistor grain boundaries above T_C , EBIC may be observable in commercial devices under these conditions. However, prior to this study, EBIC has only been reported in a model thermistor system based on Nb-doped BaTiO₃ with a 3 mm grain size.¹³

In this contribution the results of preliminary experiments to study the local electrical behaviour of PTC thermistors using hot stage conductive mode microscopy and related techniques are presented.

2. Method

Cross sections of commercial barium titanate based PTC thermistor pellets (GE Thermometrics Limited, UK) were prepared for conductive mode imaging by cutting and polishing using a colloidal-silica polishing medium. Pairs of titanium current collecting electrodes with an inter-electrode separation of 35 μm were deposited using a photolithographic technique. The sample was mounted on a Gatan heating stage in a

Phillips 525 SEM and imaged using the secondary, backscattered and conductive modes of operation. Grain boundary misorientations were established through electron backscattered pattern (EBSP) analysis of grain orientations using a Phillips XL30 FEGSEM operating at 20 KeV. EBSP data was processed using commercial software (HKL, Denmark).

3. Results and discussion

Fig. 2 (a) is a secondary electron (SE) image of an area of the thermistor selected for detailed study. The material has a variable grain size, with a mean value of 5.4 μm , and shows some intergranular porosity. The edges of the current-collecting electrodes are visible on either side of the image, and are spaced approximately six grain widths apart in the REBIC configuration. Fig. 2(b) is a conductive mode image of the same area, collected at 100 °C, i.e. below T_C . At this temperature no EBIC contrast is observed, suggesting the absence of charge separating electrostatic barriers at the thermistor grain boundaries under these conditions. This observation is consistent with models for PTC behaviour that predict the suppression of electrostatic grain boundary barriers below T_C by their interaction with the spontaneous polarisation of the ferroelectric phase.² When the specimen is heated to a temperature above T_C , EBIC contrast is observed at some grain boundaries. Fig. 2(c) shows a conductive mode image of the same area, collected at 180 °C. EBIC contrast is present as dark-bright contrast parallel to some grain boundaries. The dark-bright EBIC image contrast is consistent with it being formed by the collection of currents generated by the separation of primary-beam induced electron-hole pairs in the opposed space-charge fields on either side of the grain boundary plane. The EBIC image contrast observed here is similar to that generated in other electrically active wide bandgap semiconducting materials with cubic symmetry, such as ZnSe or CdTe, but differs from that commonly observed in hexagonal materials such as zinc oxide, where internal fields generated by crystal anisotropy at asymmetric grain boundaries act to suppress the EBIC from one side of the grain boundary plane.⁹ Although formed by beam interactions with the grain boundaries, the extent to which the EBIC image contrast appears to extend into the adjacent grains depends both on the imaging conditions used and on materials parameters such as the minority carrier diffusion length.

The distribution of EBIC active grain boundaries throughout the sample is not homogeneous. For example, the grain boundaries represented in the upper portion of Fig. 2(c) generally show EBIC contrast, whereas those in the lower portion do not. The reason for this difference is currently unclear but may be related to

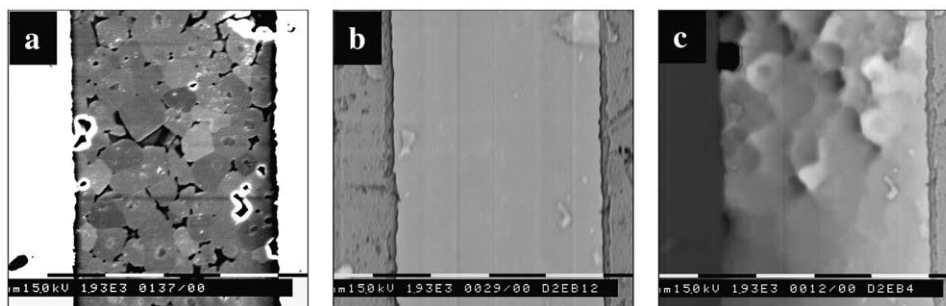


Fig. 2. (a) SE image of inter-electrode area; (b) conductive mode image of same area at 100 °C; (c) Conductive mode image at 180 °C showing EBIC contrast (scale bar = 10 μm).

changes in the grain boundary barrier structure brought about by microstructural variations arising from inhomogeneities in the local concentrations or distributions of dopants. It has also been suggested that the conditions necessary for EBIC to be generated are not met at grain boundaries where there exists a thick insulating grain boundary film, suggesting that EBIC may not occur at grain boundaries where a sufficiently high concentration of additives are present to allow a discrete second phase film to form.¹⁴

Fig. 3 shows the variation in peak EBIC current with beam current for an EBIC active grain boundary. The EBIC gain, defined as the ratio of the peak EBIC current to the incident beam current is less than unity, which is typical for electroceramics.⁹ Screening effects are not observed over this current range.

Fig. 4 (a) is a SE image of another region of the thermistor containing two electrically active grain boundaries, labelled 'A' and 'B'. EBSP analysis revealed that the lattice misorientation of grain boundary 'A' is given by a rotation of 16° about an axis close to [9,15,2] and grain boundary 'B' is given by a rotation of 45° about an axis close to [4,−1,−4]. Neither interface fell

close to a recognised low Σ coincident site lattice misorientation and so both grain boundaries may be classified as random, high angle. Fig. 4(b) is a conductive mode image of the same area, collected at 200 °C under conditions of zero applied voltage bias. Strong dark–bright contrast is visible at grain boundary 'A' but not at 'B'. The signal at grain boundary 'A' may be confirmed as EBIC by observing its behaviour under an externally applied voltage bias. When a positive [Fig. 4(c)] or negative [Fig. 4(d)] bias is applied across grain boundary 'A', the effect is to compensate the space-charge field on one side of the grain boundary plane and suppress the generation of a signal on that side of the grain boundary plane, leaving only single line EBIC contrast (Fig. 5) as has previously been reported for active grain boundaries in zinc oxide varistors.⁹ Under bias, however, grain boundary 'B' also shows bright or dark single-line contrast [Fig. 4(c) and (d)], although the lack of visible EBIC contrast when the bias is removed [Fig. 4(b)] suggests that the electrical activity observed at grain boundary 'B' under bias is instead be due to β -conductivity. The distinct forms of conductive mode contrast observed at these two grain boundaries

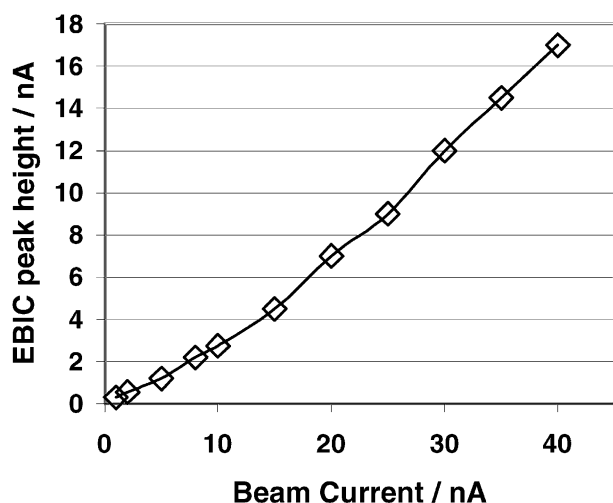


Fig. 3. Variation of EBIC current with incident beam current at an EBIC active grain boundary.

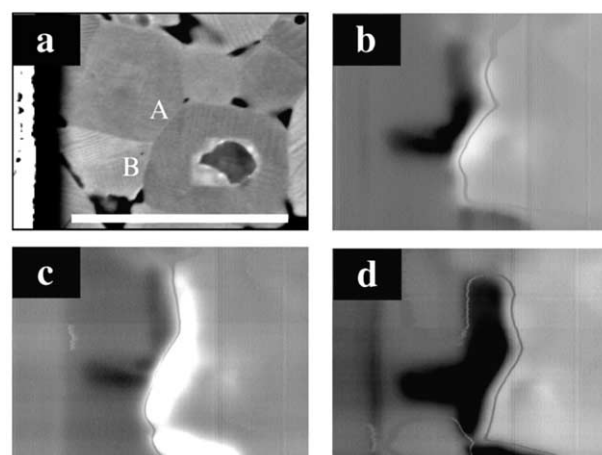


Fig. 4. (a) SE image showing two electrically active grain boundaries; 'A' & 'B'; (b–d) conductive mode images of boundaries at 200 °C under conditions of zero applied voltage bias (b), +0.5 V bias (c), and −0.5 V bias (d) (scale bar = 5 μm).

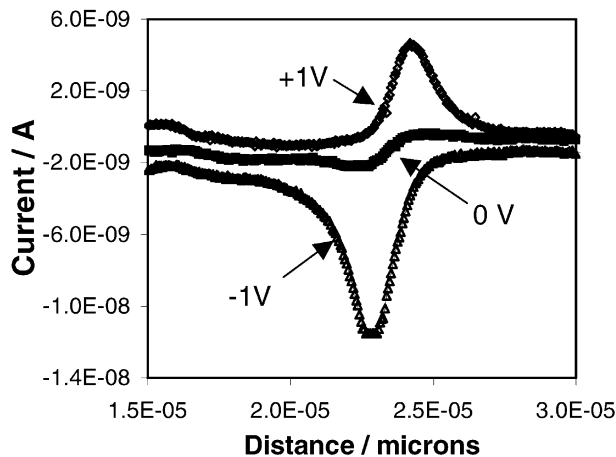


Fig. 5. EBIC current linescans across boundary 'A' showing the change in EBIC under different voltage bias conditions.

(EBIC and β -conductivity) reflect differences in the electrical structures of the two interfaces. Whilst charge separation effects in the space charge regions of grain boundary 'A' yield EBIC, which is consistent with the presence of a charge separating electrostatic barrier, in the case of grain boundary 'B' the presence of β -conductivity contrast suggests that the dominant electrical characteristic here is the caused by a resistive layer with a conductivity that is sensitive to the injection of mobile charge carriers by the electron beam. Thus, conductive mode microscopy, including bias studies, has revealed clear differences in grain boundary contrast, that reflect variations in the structure of individual thermistor grain boundaries. A detailed study of the factors giving rise to these differences is currently underway.

4. Conclusions

Conductive mode EBIC contrast has been observed for the first time in a commercial PTC thermistor. The contrast became visible at some grain boundaries as the thermistor was heated above its Curie temperature, allowing electrostatic grain boundary barriers to form. Below T_C no EBIC was observed. Some grain boundaries remained EBIC inactive above T_C , but may show β -conductivity contrast.

Acknowledgements

JS is grateful to GE Thermometrics (UK) Ltd and the EPSRC for financial support during this project.

References

- Heywang, W., Resistivity anomaly in doped barium titanate. *J. Am. Ceram. Soc.*, 1964, **47**, 484–490.
- Jonker, G. H., Advances in Ceramics, 1, Grain boundary phenomena in electronic ceramics. *J. Am. Ceram. Soc.*, 1981, 155.
- Gerthsen, P. and Hoffmann, B., Current-voltage characteristics and capacitance of single grain boundaries in semiconducting BaTiO₃ ceramics. *Sol. Stat. Elec.*, 1973, **16**, 617–622.
- Nemoto, H. and Oda, I., Direct examinations of PTC action of single grain boundaries in semiconducting BaTiO₃ ceramics. *J. Am. Ceram. Soc.*, 1980, **63**, 398–401.
- Miki, T., Fujimoto, A. and Jida, S., An evidence of trap activation for PTCR in BaTiO₃ ceramics with substitutional Nb and Mn as impurities. *J. Appl. Phys.*, 1998, **83**, 1592–1603.
- Kuwabara, M., Morimo, K. and Matsunaga, T., Single-grain boundaries in PTC resistors. *J. Am. Ceram. Soc.*, 1996, **79**, 997–1001.
- Hayashi, K., Yamamoto, T. and Sakuma, T., Grain orientation dependence of the PTCR effect in niobium-doped barium titanate. *J. Am. Ceram. Soc.*, 1996, **79**, 1669–1672.
- Leach, C. and Russell, J. D., Problems associated with imaging resistive barriers in BaTiO₃ PTC ceramics using the SEM conductive mode. *J. Eur. Ceram. Soc.*, 1995, **15**, 617–622.
- Leach, C., The effect of voltage bias on the EBIC contrast present at varistor grain boundaries. *Int. Sci.*, 2000, **8**, 375–388.
- Russell, G. J., Robertson, M. J., Vincent, B. and Woods, J., An electron beam induced current study of grain boundaries in zinc selenide. *J. Mat. Sci.*, 1980, **15**, 939–944.
- Palm, J. and Alexander, H., Direct measurement of the local diffusion length grain boundaries by EBIC without a schottky contact. *J. Phys. IV, Colloq. C6, supplement to J. Phys. III*, 1991, 101–106.
- Leach, C. and Russell, J. D., Beta-conductivity contrast at barium titanate thermistor grain boundaries. *J. Eur. Ceram. Soc.*, 1996, **16**, 1035–1039.
- Kataoka, N., Hayashi, K., Yamamoto, T., Sugawara, Y., Ikuhara, Y. and Sakuma, T., Direct observation of the double schottky barrier in niobium-doped barium titanate by the charge collection method. *J. Am. Ceram. Soc.*, 1998, **81**, 1961–1963.
- Palm, J., Local investigation of recombination at grain boundaries in silicon by GB-EBIC. *J. Appl. Phys.*, 1993, **74**, 1169–1178.